

Ising-model Monte Carlo simulations: Density of states and mass gap

Nelson A. Alves, Bernd A. Berg, and Ramon Villanova

*Department of Physics and Supercomputer Computations Research Institute, The Florida State University,
Tallahassee, Florida 32306*

(Received 7 June 1989)

We have performed Monte Carlo simulations for the three-dimensional Ising model. Using histogram techniques, we calculate the density of states on L^3 block lattices up to size $L = 14$. Statistical jackknife methods are employed to perform a thorough error analysis. We obtain high-precision estimates for the leading zeros of the partition function, which, using finite-size scaling, translate into $\nu = 0.6285 \pm 0.0019$. Along a different line of approach following recent work in lattice-gauge theories, we accurately determine the mass gap $m = 1/\xi$ (ξ correlation length) for cylindrical L^2L_z lattices (with $L_z = 256$ and L up to 12). The finite-size-scaling analysis of the mass-gap data leads to $\nu = 0.6321 \pm 0.0019$.

I. INTRODUCTION

Although not solved exactly, the 3D Ising model is certainly one of the well-understood systems in modern statistical mechanics. Still being interesting on its own, it is in addition a suitable testing ground for new numerical techniques and ideas. In the present paper we rely on "old fashioned" Monte Carlo (MC) methods to generate Ising-model configurations and employ new methods to extract physics from these configurations. Periodic boundary conditions are consistently used. In the first part we concentrate on computing the Lee-Yang¹ zeros of the partition function. The second part is concerned with calculating the ratio of the two largest eigenvalues of the transfer matrix or, equivalently, the mass gap of the system. In both cases finite-size scaling theory (FSST)²⁻⁴ leads us to estimates of the critical exponent ν that are competitive with the best results in previous literature.

In this paper we are concerned with investigations of finite systems. The density of states $\rho(E)$ is defined by

$$Z(\beta) = \sum_E \rho(E) \exp(-\beta E), \quad (1.1)$$

where $Z(\beta)$ is the partition function and the summation goes over the allowed energy values of the system. Once the density of states is known, the zeros of the partition function can be studied, a problem which has received a lot of attention for quite a while.^{5,6} Various methods for calculating the density of states have been presented in the statistical mechanics literature and were applied to small systems. So called "histogram" methods have turned out to be efficient. Reference 7 summarizes early original contributions of relevance and the interested reader may consult Ref. 8 for a more detailed presentation of the history. To our knowledge the first corresponding MC investigation of partition function zeros was carried out by Marinari and collaborators.^{9,10} Recently, renewed interest in the subject was stimulated by Bhanot *et al.*^{11,12} who commend the use of the Creutz¹³ demon variant of the microcanonical approach. Presumably prompted by this work, MC methods of the type ex-

plored in Refs. 7, 9, and 10 were rediscovered and refined by Ferrenberg and Swendsen.¹⁴

The original papers⁷⁻¹⁰ certainly deserve their well-earned credit, but we would like to mention that none of them actually played a role for the progress of the work presented here. Instead, our investigation has its own little history. The actual starting point was some uneasy feeling about the efficiency of the method of Bhanot and collaborators.¹¹ From a numerical study of random surfaces¹⁵ one of the present authors already had experience with a MC histogramming method. In addition, previous work with jackknife methods^{16,17} turned out to be useful for developing an efficient "patching" procedure, to calculate the density of states by joining several histograms. Now we realize that much of that was anticipated earlier.⁷ Without this knowledge our work progressed rather straightforwardly and naturally. By the middle of 1988, most of the data for the first part of this paper were taken,¹⁸ and the obtained density of states had been quantitatively compared with results from Refs. 11 and 12; the analysis of the zeros and the second part of the paper were still missing by that time. After completion of our work we became aware of the paper by Ferrenberg and Swendsen¹⁴ that had the positive effect of drawing a lot of attention to the histogramming methods themselves and to stimulate a quite "successful" search for original literature.

Although details of the employed method are certainly a bit tricky, we would like to concentrate first of all on the obtained final estimate for the critical exponent ν . The tremendous improvement on the scale of Marinari's work¹⁰ seems not only to be due to patching and modern computer resources, but possibly also due to our way of averaging over short-range fluctuations (see Sec. II A). Superficially the improvement looks less dramatic in comparison with Ref. 12. However, our method allows us rather easily to reach L^3 lattices with L as big as 14. The largest lattice treated so far (with abundant computer resources) was $L = 10$,¹² and Marinari's investigation¹⁰ ran already at $L = 8$ into trouble. It should be remarked that statistical jackknife methods (see for instance Refs.

16 and 17) are efficient for calculating reliable statistical error bars for the density of states, the partition function zeros, and ν .

Along our second line of approach, we calculate directly the relevant correlation length ξ on finite systems and estimate ν by applying FSST to it. Typically, one is interested in the ratio

$$\lambda = \frac{\lambda_1}{\lambda_0}, \quad (1.2)$$

where λ_0 is the largest and λ_1 the next largest eigenvalue of the transfer matrix. Then one has

$$\xi^{-1} = m = \ln \lambda, \quad (1.3)$$

where m is the mass gap of the system. (This is standard use for m in field theory. In statistical mechanics m normally denotes the spontaneous magnetization, which is not investigated in this paper.) In two dimensions the transfer-matrix approach (TMA) has successfully provided the desired finite volume results for various systems.³ However, it seems that generalizations of the TMA to higher dimensions are rather limited because of the prohibitively fast increase of the matrix size with volume. One purpose of this paper is to draw attention to the fact that MC calculations of the type pioneered in mass spectrum computations of lattice-gauge theories^{19,17} allow us to calculate the ratio $\lambda = \lambda_1/\lambda_0$ directly and sufficiently accurate. One may call this Monte Carlo transfer matrix method (MCTMA). The masses calculated by MCTMA are analyzed by FSST along the lines of a recent investigation of the deconfining phase transition in lattice-gauge theories²⁰ and result in our second estimate of ν . The simplicity of both lines of our approach, as compared to MC renormalization-group²¹ and analytical transfer-matrix³ calculations, deserves to be emphasized.

Our computer code is a modified version of Ref. 22. The program uses multispin coding and updates 64 lattices simultaneously. Statistical analysis in this paper is always with respect to the corresponding 64 results. However, to avoid correlations between these results we found it necessary (as already in Ref. 23) to use different random numbers for each of these lattices. As compared to Ref. 22, this slows down the speed of the updating by a factor of $\approx 4-5$. As Cyber 205, ETA-E, ETA-Q, and ETA-G were used, it is most appropriate to state the up-

dating time in almost machine-independent clock cycles. Rather typical is ≈ 2.1 clock cycles per spin updated on the 6^2 256 lattice. Smaller systems are slower, larger systems tend to be somewhat faster. In Cyber 205 equivalents our complete computer time spent was about 100 h for the partition function study, half of this time for the $L=14$ lattice, and about 380 h for the mass-gap investigation.

Let us conclude the introduction with a short outline of the paper. Section II is concerned with our numerical evaluation of the partition function. Section II A describes in detail how our MC calculation of the density of states is performed. In Sec. II B our partition function zeros are then calculated and, together with results from previous literature,¹² they are used to give our first estimate of ν . In Sec. III the MCTMA results are presented. Besides the 3D Ising model, the 2D Ising model is also treated for illustrative purposes. Section III A summarizes the crucial aspects of our numerical mass calculations and gives a table of our most accurate mass estimates. Section III B collects the relevant finite-size-scaling formulas and carries out the analysis that leads to β_c and ν . A brief outlook and conclusion are given in Sec. IV.

II. MONTE CARLO CALCULATION OF THE PARTITION FUNCTION

In this section we consider the 3D Ising model in the L^3 block geometry. The energy is given by

$$E = -\frac{1}{4} \sum_{\langle ij \rangle} s_i s_j, \quad s_i = \pm 1. \quad (2.1)$$

Here the normalization is chosen such that E changes in increments of 1, and for L even,

$$-3L^3/4 \leq E \leq +3L^3/4.$$

For the density of states (1.1) the normalization

$$\sum_E \rho(E) = 2^{L^3} \quad (2.2)$$

holds.

In the following we report MC calculations for the density of states. Typically they rely on $2.75 \cdot 10^5$ or $4 \cdot 10^5$ sweeps per data point and in addition 6000 to 20000 sweeps are discarded for reaching equilibrium. A data point is defined by lattice size and β value, i.e., (L, β) . Because of multispin coding we have each data point in a multiplicity of 64 lattices. The list of data points is

$$(L=6: \beta=0.19, 0.22165, 0.255),$$

$$(L=8: \beta=0.193, 0.22165, 0.24),$$

$$(L=10: \beta=0.05, 0.10, 0.15, 0.195, 0.22165, 0.235, 0.25, 0.275, 0.30, 0.34, 0.38),$$

and

$$(L=14: \beta=0.165, 0.19, 0.20, 0.215, 0.22165, 0.225, 0.228, 0.235).$$

A. Density of states

The MC Markov chain generates configurations $K = \{s\}$ with the Boltzmann weight

$$P(\{s\}) = e^{-\beta E(\{s\})}.$$

One may now histogram the generated configurations with respect to the energy E . It turns out that these histograms are noisy because of short-range fluctuations. This problem was sufficiently suppressed by adding one entry for each energy change of one-eighth of the lattice. In other words, we performed eight measurements per sweep. Let us denote the number of entries with energy E by $h_{MC}^i(E)$. Clearly,

$$\rho_{MC}^i(E) = c^i h_{MC}^i(E) \exp(+\beta_i E) \quad (2.3)$$

is an estimator for the density of states defined by (1.1). Here the superscript i serves to keep track of the variant β values and one may adjust the free constant c^i such that (2.2) is fulfilled. For the special case of using long MC runs at single β values, the density of states was estimated this way in Ref. 10. To give an example, we depict in Fig. 1 the histogram h_{MC} at $\beta=0.22165 \approx \beta_c$ for our largest lattice ($L=14$). It is questionable whether the resulting ρ_{MC} is sufficiently precise to allow an acceptable estimate of partition function zeros (see Sec. II B). To overcome this difficulty, we decided to patch results ρ_{MC}^i corresponding to variant β values. Again for $L=14$, Fig. 2 depicts our complete set of “raw” histograms $h_{MC}^i(E)$ with, in this case, $i=1, \dots, 8$. It is worthwhile to describe the patching procedure in some details. Due to the multispin coding we have 64 independent histograms h_{MC}^{ij} ($j=1, \dots, 64$) for each i . By multiplication with the appropriate Boltzmann factors we define a set of

$$\rho_{MC}^{ij}(E) = h_{MC}^{ij} \exp(+\beta_i E), \quad (2.4)$$

which differ from the corresponding ρ_{MC}^{ij} only by the multiplicative constants c^{ij} . We want to combine the

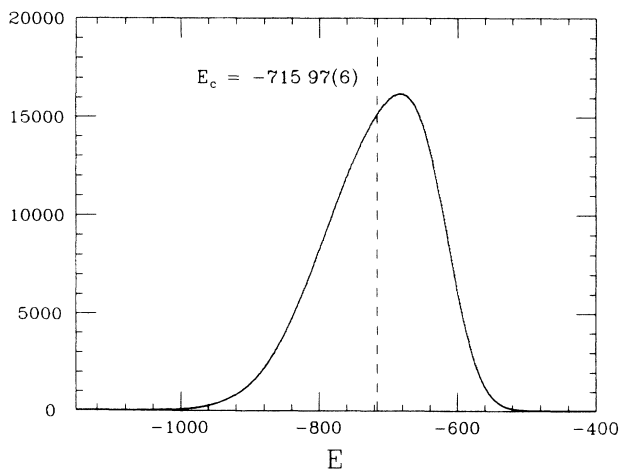


FIG. 1. Histogram for $\beta=0.22165$ and $L=14$. For each energy the number of entries found in our MC simulation is given. The value $E_c = \langle E \rangle_{\beta=\beta_c}$ indicates the mean energy for this distribution.

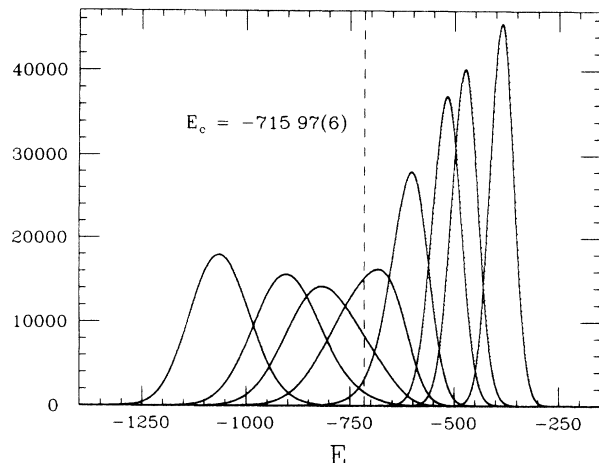


FIG. 2. All eight histograms for our 14^3 lattices. The value $E_c = \langle E \rangle_{\beta=\beta_c}$ is also indicated.

$\rho_{MC}^{ij}(E)$ to one estimator $\rho_{MC}(E)$ for the density of states $\rho(E)$. Let us first spare out the question of error propagation. Mean values and their errors bars are defined by

$$\rho_{MC}^i(E) = \frac{1}{64} \sum_{j=1}^{64} \rho_{MC}^{ij}(E) \quad (2.5)$$

and

$$\Delta \rho_{MC}^i(E) = \left[\frac{1}{64} \sum_{j=1}^{64} (\rho_{MC}^{ij} - \rho_{MC}^i)^2 \right]^{1/2}. \quad (2.6)$$

Subsequent patches overlap. Using least-squares fitting, we may combine the ρ_{MC}^i . This is done by recursively calculating constants c^{i+1} ($c^1=1$, $i=1, 2, \dots$) such that

$$\sum_{E \in \text{overlap}} \frac{[c^i \rho_{MC}^i(E) - c^{i+1} \rho_{MC}^{i+1}(E)]^2}{[c^i \Delta \rho_{MC}^i(E)]^2 + [c^{i+1} \Delta \rho_{MC}^{i+1}(E)]^2} = \min. \quad (2.7)$$

After all the constants c^i are determined, we define a combined $\rho'_C(E)$ by means of

$$\rho'_C(E) = \frac{\sum_i w^i(E) c^i \rho_{MC}^i}{\sum_i w^i}, \quad (2.8)$$

where the weight factors w^i are given by

$$w^i(E) = \begin{cases} [\Delta \rho_{MC}^i(E)]^{-2}, & \text{if } \Delta \rho_{MC}^i / \rho_{MC}^i < \text{cutoff}, \\ 0, & \text{if } \Delta \rho_{MC}^i / \rho_{MC}^i \geq \text{cutoff}. \end{cases} \quad (2.9)$$

$\rho'_C(E)$ determines the desired estimator $\rho_{MC}(E)$ up to an overall constant, which is fixed by Eq. (2.2).

A few remarks are in order. (i) The results obtained depend slightly on the chosen order of the patches. It is recommendable to take $\beta_1 \approx \beta_c$ and to alternate from there on such that the β_i (i even) are on one side and the β_i (i odd) are on the other side of β_1 . (ii) Towards small

as well as large E our cutoff criterium was to stop whenever a single entry of one of the two patches had for the first time an error of more than 10%. We obtained the same results with the choice 50%. Some kind of cutoff is necessary. Admitting, too, unreliable boundary regions would spoil the whole procedure. In the extreme limit of energies with no entries into the histogram also the error bar $\Delta\rho_{MC}^i(E)$ becomes zero. This is a rather typical case of a bias problem. (iii) Data and, consequently, error bars within one histogram are strongly correlated. This deprives the χ^2 of the fits of their statistical meaning in the sense of confidence levels, but χ^2 is still supposed to determine reliably the maximum likelihood estimate of c^{i+1} . (iv) Multiple overlaps are taken into account by our procedure, because after merging two histograms the result reflects the combined statistics of both. This is nice, as the precise overlap is only known after actually doing simulations.

Let us now turn to the problem of error propagation. The obvious idea is to repeat the earlier construction for each of the 64 lattices, i.e., starting off with $h_{MC}^{i,j}(E)$ (j fixed). We have to assign error bars to the $\rho_{MC}^{i,j}(E)$, otherwise we cannot carry out the patching. The only choice is $\Delta\rho_{MC}^{i,j}(E) = 8\Delta\rho_{MC}^i(E)$, independent of j , and the factor 8 might make the bias problem of remark (ii) severe. A nonrecommendar approach would be to carry out partial sums over some of the lattices and to reduce the number of samples to, say, four. This would still mean a factor of 2 for the error bar and, in addition, with only four samples the student distribution (see for instance Refs. 24 and 17) deviates significantly from a Gaussian distribution. With the limited statistics of a realistic simulation the jackknife method provides the better solution. Then, there is never a reason to work with an artificially small number of samples and, as a rule of thumb, 20 is a good number; see Ref. 17 for a more detailed discussion. For our present investigation 64 is, of course, the obvious choice and jackknife samples are defined by

$$h_j^k(E) = \frac{1}{63} \sum_{j \neq k} h_{MC}^{i,j}(E), \quad k = 1, \dots, 64. \quad (2.10)$$

Corresponding $\rho_j^{i,k}(E)$ follow by the analog of Eq. (2.4). The error bar $\Delta\rho_j^{i,k}(E)$ can either be calculated directly, or independent of k be defined as $\sqrt{64/63}\Delta\rho_{MC}^i(E)$. We have checked that both ways give fully compatible re-

sults. Now, we carry out the patching procedure 64 times, once for each of the jackknife samples, resulting in 64 estimators $\rho_j^k(E)$ ($k = 1, \dots, 64$) for the density of states. Of course, $\rho_{MC}(E)$ is still the best estimate. Its error bar is now given by the jackknife formula

$$\Delta\rho_{MC}(E) = \left[\frac{63}{64} \sum_{k=1}^{64} [\rho_{MC}(E) - \rho_j^k(E)]^2 \right]^{1/2}. \quad (2.11)$$

In the limit of no bias this definition is identical with the usual error bar, but for biased situations the jackknife error bar is by far more reliable. Proceeding further one may compute arbitrary functions

$$f_j^k = f(\rho_j^k(E_1), \rho_j^k(E_2), \dots) \quad (2.12)$$

for each jackknife sample as well as for the complete statistics. The latter result is denoted f_{MC} and the analog of Eq. (2.11) holds for the error Δf_{MC} . This is how we calculate the statistical errors of our partition function zeros. In a last step, the bias B itself may be estimated as

$$B(f_{MC}) = -63 \left[f_{MC} - \frac{1}{64} \sum_k f_j^k \right]. \quad (2.13)$$

In a reliable MC simulation the bias should be negligible as compared with the statistical error. Otherwise one may correct for the bias, but faces increasing difficulties when one tries to estimate the errors of such corrections. In the present investigation we did not encounter any serious bias problems.

To complete this section let us mention that we set out to replace the simple MC measurements by sampling the $2^{N/2}$ independent configurations of each checkerboard. Using standard convolution formulas (see for instance Ref. 24), this is straightforward but tedious. We hoped to gain by the enormous number of $2^{N/2}$ configurations sampled each time this way. This hope turned out to be unjustified.¹⁸ The thus sampled configurations were noisy and strongly correlated. The needed large, additional amount of computer time for measurements never paid off.

B. Partition function zeros

Defining

$$u = \exp(-4\beta), \quad (2.14)$$

TABLE I. First partition function zero. Due to reasons explained in the text, we have multiplied the error bars of Ref. 12 by a factor of 3. For $L = 3$ and 4 the entries are exact results.⁵ Their weights in the fits are determined by assigning an error of 1 to the last given digit.

L	This paper		Reference 12	
	$\text{Re}(u_1^0)$	$\text{Im}(u_1^0)$	$\text{Re}(u_1^0)$	$\text{Im}(u_1^0)$
3	0.365 053 . . .	0.141 742 . . .		
4	0.384 283 . . .	0.087 739 . . .		
5			0.392 787(15)	0.060 978(15)
6	0.397 578(18)	0.045 443(16)	0.397 563(15)	0.045 411(15)
8	0.402 728(17)	0.028 604(14)	0.402 718(15)	0.028 596(15)
10	0.405 395(16)	0.020 006(15)	0.405 405(15)	0.019 996(15)
14	0.408 078(09)	0.011 673(09)		

TABLE II. Convergence of the patching procedure for the 14^3 lattice.

Number of patches	First zero		Second zero	
	$\text{Re}(u_1^0)$	$\text{Im}(u_1^0)$	$\text{Re}(u_2^0)$	$\text{Im}(u_2^0)$
1	0.408 063(14)	0.011 703(11)	0.400 81(14)	0.015 12(13)
3	0.408 075(09)	0.011 678(10)	0.394 51(11)	0.015 60(12)
5	0.408 078(09)	0.011 672(09)	0.402 96(08)	0.018 33(08)
8	0.408 078(09)	0.011 673(09)	0.402 93(08)	0.018 27(08)

the partition becomes a polynomial of degree $3L^3/2+1$ in u (we only consider L even). Its coefficients are determined by the spectral density, numerically calculated in the previous section. Using the Newton-Raphson method, as described in Ref. 25, we calculated the first few zeros which are closest to the infinite volume critical point. The results for the first zero u_1^0 are given in Table I. The relevance of our patching procedure is illustrated by means of Table II. For our largest lattice we give the dependence of the first and second zero on the number of patches. For the special case of one patch errors due to bias are clearly visible. From three samples on these errors are of the same order of magnitude as the statistical error bars. For five samples, convergence is already satisfactory. Clearly, the convergence is better for the first than for the second zero. There are still reasonable results for the third zero, but for subsequent zeros higher statistics and more patches would be needed. It is remarkable that, in contrast to the claims of Ref. 10, already for one patch the results for the first zero are quite reasonable. This is even more astonishing in view of the large lattice size $L=14 \gg 8$. Likely, it is related to our way of suppressing the noise of short scale fluctuations.

The calculation of zeros was repeated 64 times, once for each jackknife sample. This analysis yields the reported error bars. Calculating, instead, the error bars by applying the Gaussian model of Ref. 11 to our data gives values approximately three times smaller. The difference is due to the already mentioned correlation of the data within one histogram. This casts some doubts on the error analysis of Ref. 12. As in their approach each histogram has only four entries, one may argue that the effect is presumably less pronounced. The correlations between entries within one histogram would be described by the 4×4 covariance matrix.²⁴ The essence is that the correct error bars for the zeros of Ref. 12 can only be recovered by producing at least some new data with their method. The conservative approach is to multiply their reported errors by a factor of 3. This is supposed to be a reliable upper bound, and is in accordance with the error correction done in Ref. 12 for the final estimate of ν . For the convenience of the reader, we include the thus modified results of Ref. 12 in Table I. The thus collected data are slightly overconsistent with one another. This might hint towards too large error bars, but with only three independent samples to compare ($L=6, 8, 10$) a thorough analysis is hardly possible. The statistically weighted average from the joint data set is now used to estimate ν .

Let us define $u_c = u(\beta_c)$ and carry out the FSS analysis

for the first zero. It is well known⁶ that for sufficiently large L

$$u_1^0(L) = u_c + AL^{-1/\nu}[1 + O(L^{-\omega})], \quad \omega > 0. \quad (2.15)$$

In first approximation this is reflected by the linear regression

$$-\ln|u_1^0(L) - u_c| = \text{const} + \frac{1}{\nu} \ln(L). \quad (2.16)$$

We use the accurate estimate (Ref. 21) $u_c = 0.412047 \pm 0.000010$ and depict in Fig. 3 the corresponding two parameter fit of the $L \geq 4$ zeros. Although the straight-line behavior is very impressive, it is pointless to judge the quality of this fit by eye. The invisible reason is the high precision of our data. As a matter of fact, the “goodness” Q of this fit is zero (more precisely $< 10^{-17}$). Figure 3 is obtained relying on the Fortran subroutine FIT of Ref. 25. In addition to the maximum likelihood fit and its associated errors, this subroutine calculates χ_{expt}^2 and the probability Q that the χ^2 value of an appropriately defined normal distribution could exceed χ_{expt}^2 . Q is a standard measure for the goodness of a fit, and in the average $Q=0.5$. Consequently, the likelihood that our zeros are well described by the straight-line fit (2.16) is for all practical purposes zero and the ν estimate of Fig. 3 has to be discarded.

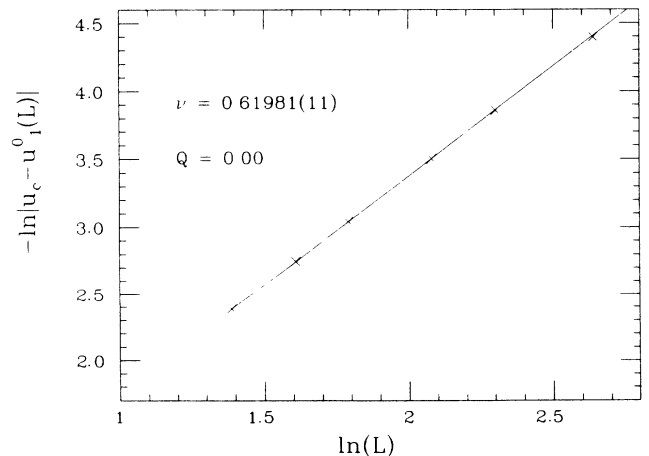


FIG. 3. Linear regression for $-\ln|u_1^0(L) - u_c|$ in the range $L=4-14$.

TABLE III. Determination of ν by linear regression.

L	ν	$ u_0^1 - u_c $	Results from $\text{Im}(u_1^0)$	
			ν	Q
(4,5,6,8,10,14)	0.6198(2)	$< 10^{-17}$	0.6184(2)	$< 10^{-17}$
(5,6,8,10,14)	0.6248(3)	10^{-10}	0.6221(3)	10^{-7}
(6,8,10,14)	0.6260(3)	0.02	0.6231(3)	0.02
(8,10,14)	0.6274(6)	0.90	0.6244(6)	0.66

How can we do better? The straightforward way is by omitting the smallest lattices, responsible for the largest finite-site corrections, from the linear regression. In that way one obtains the ν values of Table III and their corresponding Q 's. Omitting successively $L=4, 5$, and 6 improves the goodness of the fit. With only $L=8, 10$, and 14 left, the straight-line fit is self-consistent. Obviously, for the remaining section of the straight line the finite-size corrections are overwhelmed by the statistical noise. It is interesting to note the systematic increase of the ν 's of Table III. The accuracy of the zeros from Table I suggests to try multi-parameter fits for estimating the finite-size corrections explicitly. Following Ref. 12 we carry out the four parameter fit

$$|u_1^0(L) - u_c| = a_1 L^{-1/\nu} + a_2 L^{-a_3}. \quad (2.17)$$

Including $L=3$ we already find $Q=0.93$ and, on the scale of the previous figure, the fit and its resulting ν estimate are depicted in Fig. 4. The corresponding exponent a_3 is $a_3 = 4.86 \pm 0.12$. Although the goodness of the fit cannot improve, it seems advisable to omit the exact $L=3$ and $L=4$ results from the final estimate, as their assumed precision may obscure the accuracy of the final estimate and may give an overweight to the least relevant region. In this way we obtain

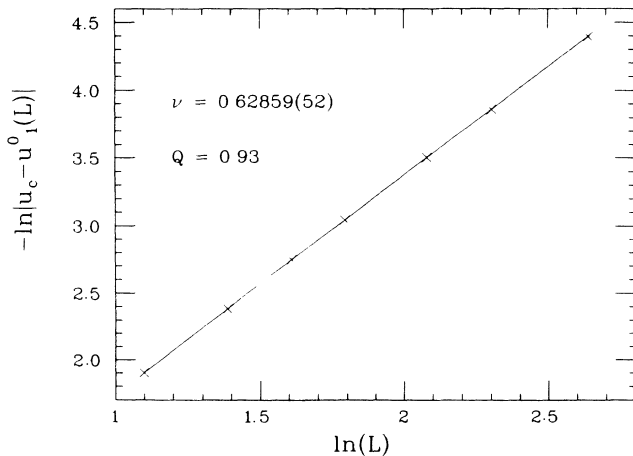


FIG. 4. Four parameter fit for $|u_1^0(L) - u_c|$ in the range $L=3-14$.

$$\nu = 0.6285 \pm 0.0019, \quad (2.18)$$

with a corresponding $a_3 = 4.7 \pm 1.9$. Of course, multi-parameter fits tend to become unstable with diminishing accuracy of the data. In that case one has to fall back to extrapolating the asymptotic estimate from the values of Table III.

In case of the 3D Ising model u_c is known with high precision. For many models of interest this is not true and one better relies on $\text{Im}(u_1^0)$. Replacing $|u_1^0 - u_c|$ by $\text{Im}(u_1^0)$, and repeating the previous analysis, we arrive at the numbers in the fourth column of Table III. The encountered differences with the numbers in the second column may serve as an indicator for the systematic errors still to be expected. It would, however, be a mistake to average over both columns of results as the absolute value already takes the appropriate average over real and imaginary parts of u_1^0 . Finally, for the sake of completeness we collect our results for the second and third zero in Table IV.

III. MONTE CARLO MASS-GAP CALCULATIONS

The MCTMA of this section is carried out on a cylindrical $L^2 L_z$ geometry ($L=4, 6, \dots, 12$), where by practical limitations $L_z=256$ approximates $L_z=\infty$. To achieve accurate correlation length estimates, it is relevant to keep one direction of the lattice as long as possible. In principle one may estimate the correlation length ξ from plain spin-spin correlations $\langle s_i s_j \rangle$. In practice, however, this is not a suitable method as the power law corrections to the asymptotic falloff of the correlation function would severely spoil the accuracy of the obtained estimates. In contrast, zero-momentum spin-spin correlation functions exponentiate. To our knowledge this was first noticed in the context of a lattice-gauge theory strong coupling investigation,²⁶ and soon after was exploited for MC glueball calculations.¹⁹ The zero-momentum spin is defined by

$$S_z = \sum_{x,y} s_{x,y,z}, \quad \text{where } (x,y) \in L^2, \quad (3.1)$$

and we have

$$C(z) = \langle S_0 S_z \rangle \sim \left[\frac{\lambda_1}{\lambda_0} \right]^z = \exp(-mz), \quad \text{for } z \rightarrow \infty \quad (3.2)$$

for the large distance behavior of the zero-momentum correlation function $C(z)$. Relying on the transfer-matrix formalism, a detailed discussion is given in Ref. 17.

A. From correlation functions to mass-gap estimates

We have assembled a small, illustrative data set for the toy case of the 2D Ising model and three large data sets for the 3D Ising model. We shall describe in detail the results obtained from the largest data set. In that case each (L, β) data point relies on 128 000 sweeps plus an additional 16 000 discarded sweeps for reaching equilibrium. Of course, we have these statistics in a multiplicity of 64 independent lattices per data point. The other two 3D Ising model data sets are more of exploratory character. The first relies on 32 000 sweeps (plus 4000 for equilibrium) per data point and the corresponding numbers for the second data set are 32 000 sweeps (plus 8000 for equilibrium). The second data set was taken to check into questions about equilibration and random numbers. With the experience of the first two data sets we decided about appropriate lattices and β values for the long runs. The estimates of the critical exponent ν are consistent for all three data sets. Therefore, we shall include the statistics gained by the “exploratory” runs in the final estimate. For the 2D Ising model we assembled data points on $L \cdot 1024$ ($L=4, 6, \dots, 12$) lattices with statistics of 16 000 sweeps (plus 2000 for equilibrium) each.

Our MC estimator $C_{MC}(z)$ for $C(z)$ is obtained by measuring $S_{z_1} S_{z_2}$ with distance $d(z_1, z_2) = z$ every 10 sweeps. Here, the distance function $d(z_1, z_2)$ takes care of the periodic boundary conditions and the average over all z_1, z_2 with $d(z_1, z_2) = z$ is performed. Once the zero-momentum correlation functions are numerically known,

$$\frac{C_{MC}(z)}{C_{MC}(z-1)} = \frac{\exp[-m(z)z] + \exp[-m(z)(L_z - z)]}{\exp[-m(z)(z-1)] + \exp[-m(z)(L_z - z + 1)]} \quad (3.3)$$

For $\beta=0.2215$, Fig. 5 gives a visual impression of the effective masses belonging to the large statistics data set. Already at fairly short distances, the effective masses $m(z)$ become, within their error bars, indistinguishable from the asymptotic value $m = m(\infty)$. With an appropriately chosen value z_0 , a single effective mass $m(z_0)$ will serve as our estimator for m . Experience shows that in practice no or little improvements are obtained when

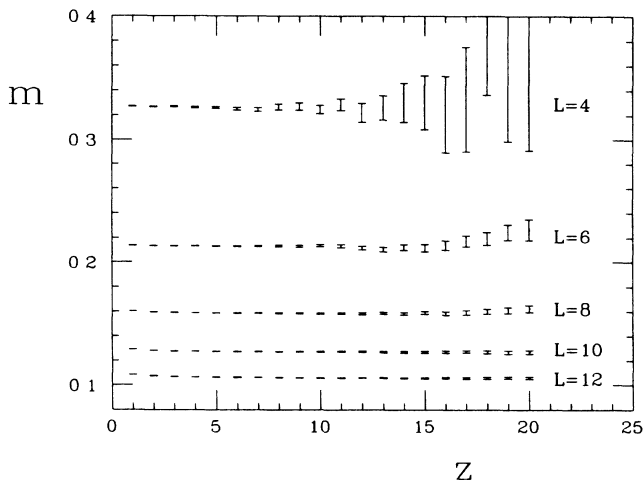


FIG. 5. Effective masses at $\beta=0.2215$. High statistics simulations are done on $L^2 256$ lattices as explained in the text.

mass-gap estimates still face serious difficulties. As a matter of fact, with the present state of the art a certain amount of subjectivity cannot be eliminated. Recently a data analysis package that does the spectroscopic analysis of correlation functions entirely on statistical grounds has been developed.²⁷ With our present data we did tests of this package and found that it still suffers from a number of instabilities and, when many data sets from variant β values are available, it cannot yet beat the human experience. Therefore, we essentially follow in this paper the pragmatic approach of Ref. 17.

Effective masses $m(z)$ at distance z are defined by the fit

one incorporates information from a whole z range by means of a suitable fitting procedure. The reason is that subsequent $m(z), m(z+1)$, etc., are strongly correlated, as is obvious from Fig. 5. A subtle issue is the choice of z_0 . This is what still brings in the subjective aspects. The following rules serve to determine z_0 . (i) As a first guess z_0 should be chosen such that $m(z_0)$ is the first effective mass that is statistically consistent with the rest, this

TABLE IV. Second and third partition function zeros (MC results of our simulation only).

L	Second zero		Third zero	
	$\text{Re}(u_2^0)$	$\text{Im}(u_2^0)$	$\text{Re}(u_3^0)$	$\text{Im}(u_3^0)$
6	0.377 59(09)	0.072 73(10)	0.3626(06)	0.0944(06)
8	0.390 07(12)	0.045 32(11)	0.3823(15)	0.0610(14)
10	0.396 61(13)	0.031 92(14)	0.3911(09)	0.0392(09)
14	0.402 93(08)	0.018 27(08)	0.3962(05)	0.0217(05)

means all masses $m(z)$ with $z \geq z_0$. (ii) For theories with positive definite transfer matrix (like Ising models) the exact effective masses have to decrease with increasing z . By statistical fluctuations an actual increase of $m(z)$ with z may happen. Whenever this happens, it signals that the statistical accuracy does not allow to determine the correction we are after and it is pointless to choose z_0 (much) further out. (iii) A spurious decrease of $m(z)$ with increasing z is more difficult to diagnose. Besides of possibly being real, it is more likely a finite-size effect because of too short a lattice length in the L_z direction.¹⁷ In the latter case, going too far out with z_0 may give a disastrous underestimate of m . (iv) Altogether, most important for choosing z_0 is to establish a stable and consistent overall pattern for the complete data set. Ingredients of this pattern are the rules

$$z_0(\beta_2) \geq z_0(\beta_1) \text{ for } \beta_2 > \beta_1 \text{ and } L \text{ fixed} \quad (3.3a)$$

and

$$z_0(L_2) \geq z_0(L_1) \text{ for } L_2 > L_1 \text{ and } \beta \text{ fixed.} \quad (3.3b)$$

In that way we obtain the mass estimates of Table V. The peculiar choices of β values and why we give

$Lm(\beta, L)$ instead of $m(\beta, L)$ are explained by the purposes of the next section.

B. Finite-size scaling analysis

It should be emphasized that we have defined the mass gap from the two-point function including the disconnected part. For the infinite system this implies

$$m(\beta) = m(\beta, \infty) = \begin{cases} > 0, & \text{for } \beta < \beta_c, \\ 0, & \text{for } \beta \geq \beta_c. \end{cases} \quad (3.4)$$

A mass \hat{m} is defined from the connected two-point function. In the disordered phase $\hat{m} = m$ because $\langle s_i \rangle = 0$, but in the infinite volume ordered phase $\hat{m} > 0$, in contrast with m . We do not calculate \hat{m} in this paper.

In finite systems, and away from the critical point $\beta = \beta_c$, we have exponentially small corrections to (3.4), which are typical for periodic boundary conditions^{4,28}

TABLE V. Mass-gap estimates for the large statistics data set: $Lm(\beta, L)$ is given. By $[z]$ we denote the distance at which the effective mass is taken to be asymptotic. Data marked by an asterisk are not used for the straight-line fits, because they lead to unacceptable Q 's.

β	$L=4$	$L=6$	$L=8$	$L=10$	$L=12$
0.2182	1.4416(24) [4]				
0.2186	1.4287(25) [4]				
0.2188	1.4188(25) [4]				
0.2190	1.4130(26) [4]	1.4710(18) [4]			
0.2192	1.3985(21) [4]	1.4555(19) [4]			
0.2194		1.4375(19) [4]	1.5294(18)* [4]		
0.2196		1.4281(18) [4]			
0.2198			1.4813(19) [4]		
0.2200			1.4555(19) [4]	1.5382(23)* [5]	1.6313(25)* [6]
0.2202			1.4298(17) [4]	1.4951(20) [5]	
0.2204				1.4655(23) [5]	1.5332(31)* [6]
0.2206					1.4855(25) [6]
0.2208					1.4417(26) [6]
0.2214					1.3064(22) [6]
0.2215	1.3057(26) [4]	1.2801(16) [4]	1.2718(17) [4]	1.2738(18) [5]	1.2766(24) [6]
0.2222					1.1211(21) [6]
0.2224					1.0787(24) [6]
0.2226				1.0900(18) [5]	1.0410(26)* [6]
0.2228			1.1197(19) [5]	1.0582(19) [5]	
0.2230			1.0926(17) [5]		
0.2232			1.0710(18) [5]		
0.2234		1.1378(14) [4]			
0.2236		1.1221(15) [4]	1.0274(16)* [5]		
0.2238	1.2171(17) [4]	1.1077(12) [4]			
0.2240	1.2070(18) [4]	1.0940(15) [4]			
0.2242	1.2028(18) [4]				
0.2244	1.1955(17) [4]				
0.2248	1.1790(16) [4]				

$$m(\beta, L) = m(\beta, \infty) [1 + O(e^{-m(\beta, \infty)L})] \text{ for } \beta < \beta_c \quad (3.5a)$$

and

$$m(\beta, L) = O(e^{-\Sigma(\beta, \infty)L}) \text{ for } \beta > \beta_c, \quad (3.5b)$$

where Σ denotes the reduced interfacial tension. For the Ising models we are dealing with second-order phase transitions. Well established finite-size scaling theory²⁻⁴

$$\frac{P(\beta, L)}{P(\beta, \infty)} = f\left(\frac{L}{\xi(\beta, \infty)}\right) \text{ (for } L \text{ large, } |\beta - \beta_c| \text{ small)}. \quad (3.7)$$

For a finite lattice there are no singularities, i.e., $P(0, L) = \lim_{\beta \rightarrow \beta_c} P(\beta, L) = \text{finite}$, and the equation

$$P(0, L) \sim \lim_{\beta \rightarrow \beta_c} \left[|\beta - \beta_c|^{-\sigma} f\left(\frac{L}{\xi(\beta, \infty)}\right) \right]$$

implies

$$f\left(\frac{L}{\xi(\beta, \infty)}\right) \sim \left[\frac{L}{|\beta - \beta_c|^{-\nu}} \right]^{\sigma/\nu} \text{ (} L \text{ constant and } |\beta - \beta_c| \rightarrow 0 \text{),}$$

as this is the only way to cancel the singular behavior of $P(\beta, \infty)$. Combining these two equations gives

$$P(0, L) \sim L^{\sigma/\nu} \text{ for } L \rightarrow \infty. \quad (3.8a)$$

Of particular importance for us are the special cases $\sigma = -\nu$ and $\sigma = 1 - \nu$

$$m(\beta_c, L) \sim L^{-1} \text{ and } \frac{d}{d\beta} m(\beta, L)|_{\beta=\beta_c} \sim L^{-1+1/\nu}. \quad (3.8b)$$

We shall compare numerical results for differently sized lattices. In case of two lattices L and L' , with $L > L'$, it

is valid in a neighborhood of the critical point. Let us consider a critical observable $P(\beta, L)$. Critical means

$$P(\beta, \infty) \sim |\beta - \beta_c|^{-\sigma}, \quad (3.6)$$

where σ is the critical exponent of P . For instance, $\sigma = \nu$ in case of the correlation length ξ . Fisher's FSS assumption is

follows from Eqs. (3.5) that $Lm(\beta, L)$ and $L'm(\beta, L')$, as functions of β , will crossover at some value $\beta = \beta_0(L, L')$, which is a fixed point of the transformation

$$\beta' \rightarrow \beta \text{ defined by } L'm(\beta', L') = Lm(\beta, L). \quad (3.9)$$

The fixed points are finite volume estimates $\beta_0(L, L')$ of the infinite volume critical coupling β_c

$$\lim_{L' \rightarrow \infty} \beta_0(L, L') = \beta_c. \quad (3.10)$$

Figure 6 summarizes our illustrative results for the 2D Ising model. The straight lines do not correspond to fits of the data, but are instead least-square fits to exact re-

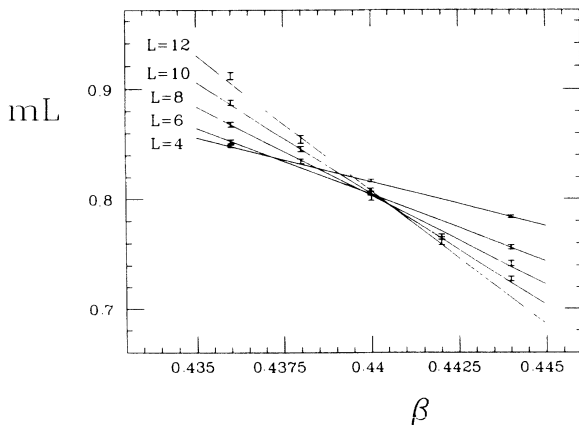


FIG. 6. MC results vs analytical results for the 2D Ising model fixed point. The straight lines are fits to the exact results.

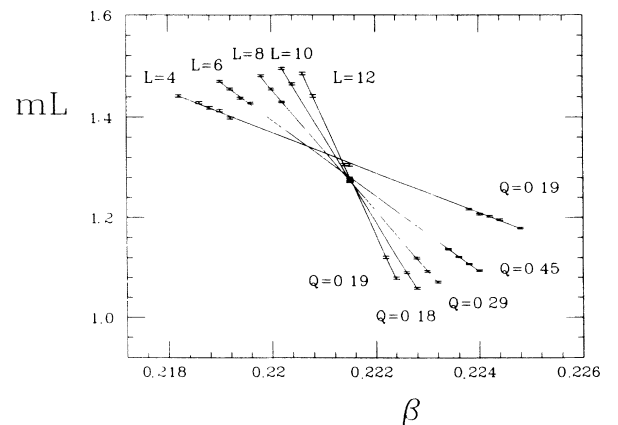


FIG. 7. MC results for the 3D Ising model fixed point. The straight lines are least-square fits to the data.

TABLE VI. 2D Ising model: estimates of $\beta_0(L, L')$. For comparison, the exact result is $\beta_c = \frac{1}{2} \ln(1 + \sqrt{2}) = 0.440\,6868\dots$

L/L'	$L=4$	$L=6$	$L=8$	$L=10$	$L=12$
4		0.437 15	0.438 43	0.439 09	0.439 48
6	0.437 03(37)		0.439 72	0.440 05	0.440 26
8	0.438 30(17)	0.439 59(40)		0.440 39	0.440 52
10	0.439 18(11)	0.440 21(19)	0.440 77(41)		0.440 66
12	0.439 55(10)	0.440 29(16)	0.440 58(26)	0.440 42(45)	

sults in the range $0.435 \leq \beta \leq 0.445$, in increments of $\Delta\beta = 0.001$, and with equal weights given to all points. In that way the analytical results reflect finite step effects due to approximating the derivative $(d/d\beta)m(\beta, L)|_{\beta=\beta_c}$ by a ratio of finite differences. The required exact masses $m(\beta, L)$ are easily computed from results in the extensive literature (see Ref. 23, and references given therein). It is a curious accident of the 2D Ising model that (3.8b) and the exact derivative of $m(\beta, L)$ at β_c give, for all L , the exact value $\nu = 1$.³ Table VI compares the analytical values for $\beta_0(L, L')$ with MC estimates. Within the statistical errors numerical and analytical results are found to be consistent. For our smallest pair of lattices ($L=6, L'=4$) the systematical error is approximately 1%, and for our largest pair of lattices ($L=12, L'=10$) it is about 100 times smaller, namely in the 5th significant digit. But in this case the statistical error is large, mainly because of the rather limited amount of computer time spent on this illustration.

Figure 7 summarizes our analogue 3D data for the large statistics data set. Now, the straight lines are least-square fits, relying on the Fortran subroutine FIT (Ref. 25). As in Sec. II B, Q indicates the quality of the fit. To increase the accuracy of the fitted lines, one would like to use β values as far apart from one another as possible. What is possible? As in Ref. 20, we answer this question by monitoring Q . As long as a straight line is a self-consistent fit to our MC data we feel on the safe side, because anyhow our data would not be precise enough to analyze the deviations. This procedure determines rather well the last admissible points. Adding more points that

are further out results often in a dramatic decrease of Q . Numbers around 10^{-6} and even smaller are not rare. For all three 3D data sets the thus obtained $\beta_0(L, L')$ estimates are given in Table VII. Altogether, the various estimates are consistent. However, the error bars of the large statistics set do not scale with $\frac{1}{2}$, as compared with either of the other two sets. Mainly responsible seem to be increased efforts to avoid all kinds of systematical errors, for instance for the asymptotic mass estimates. As a last entry in Table VII we give weighted averages over all 3D data sets. In this way our best estimate of β_c becomes

$$\beta_c \approx \beta_0(12, 10) = 0.221\,57 \pm 0.000\,03. \quad (3.11)$$

Within four significant digits this is in agreement with the most accurate results reported in previous literature, $\beta_c = 0.221\,654 \pm 0.000\,006$ (Ref. 21) and $\beta_c = 0.221\,650 \pm 0.000\,005$.²⁹ Obviously, we cannot reach this precision. Further, within its own error bar our $\beta(12, 10)$ result is inconsistent (99.4% confidence level) with these best values. It is not quite clear which systematical errors are the origin of the discrepancy. Likely, our somewhat limited lattice sizes are to blame for at least part of it. However, MC results that are significant to four or more digits are notoriously difficult to obtain and one should keep in mind the possibility of random numbers,^{17,30} rounding errors, etc., contributing. Our present investigation used the shift register random generator.³¹

By linearization around the fixed points $\beta_0(L, L')$ we estimate $(d/d\beta)m(\beta, L)|_{\beta=\beta_c}$ for various L and exploit Eq. (3.8b) to estimate ν . For our large statistics data set

TABLE VII. 3D Ising model: MC estimates of $\beta_0(L, L')$. From up to down, the first three “triangles” correspond to data sets 1–3, respectively, and the last triangle gives the weighted average.

L/L'	4	6	8	10	12
4		0.220 66(3)	0.221 03(2)	0.221 28(2)	0.221 37(2)
6	0.220 64(4)		0.221 35(3)	0.221 52(2)	0.221 53(2)
8	0.221 09(2)	0.221 45(3)		0.221 65(4)	0.221 59(2)
10	0.221 27(2)	0.221 50(2)	0.221 54(3)		0.221 54(4)
12	0.221 35(2)	0.221 51(2)	0.221 54(2)	0.221 53(4)	
4		0.220 71(3)	0.221 06(2)	0.221 24(2)	0.221 35(2)
6	0.220 69(2)		0.221 34(2)	0.221 44(2)	0.221 50(2)
8	0.221 06(2)	0.221 36(2)		0.221 54(2)	0.221 56(2)
10	0.221 25(2)	0.221 46(2)	0.221 56(2)		0.221 59(3)
12	0.221 35(2)	0.221 51(2)	0.221 56(2)	0.221 57(3)	

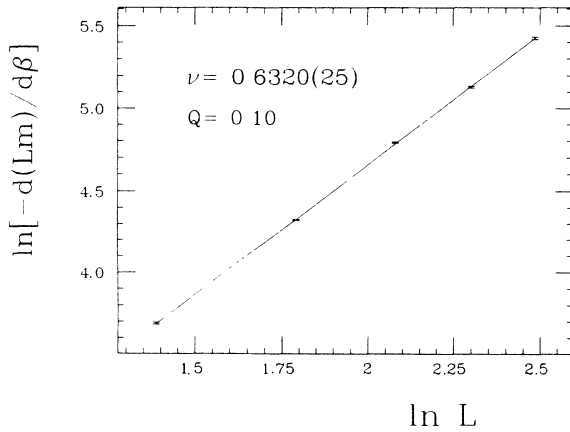


FIG. 8. Linear regression for ν by means of Eq. (3.8b).

the estimated derivatives are collected in Table VIII and the linear regression by means of Eq. (3.8b) is depicted in Fig. 8. The final Q values are in an acceptable range, but as already in Fig. 7 they fall short of the would be ideal 0.5 average. This is not really surprising, as it indicates only that our data are already precise enough to feel the involved systematical errors, mainly due to applying the straight-line fit over a finite range. In view of the often used $Q=0.05$ cut in statistical studies, we think that our range of Q values is admissible. We do certainly not care too much about systematical errors as long as they do not exceed the statistical error bars. However, as by other reasons concluded for the results of Sec. II B, we should keep this range of systematical errors in mind.

The estimate corresponding to Fig. 8 is $\nu=0.6320 \pm 0.0025$. For the other two data sets we get $\nu=0.6301 \pm 0.0033$ and $\nu=0.6344 \pm 0.0042$. Performing the appropriately weighted average, we arrive at

$$\nu=0.6321 \pm 0.0019. \quad (3.12)$$

It should be remarked that finite-size corrections to the linear regression for ν seem to be smaller in case of the mass gap than for the partition function zeros. Using our MC data for the 2D case along the same lines, the numer-

TABLE VIII. Estimates of $(d/d\beta)m(\beta, L)|_{\beta=\beta_c}$ as obtained from Fig. 7.

L	$\frac{d}{d\beta}m(\beta, L) _{\beta=\beta_c}$	Q
4	-39.98(24)	0.19
6	-75.57(26)	0.45
8	-120.41(49)	0.29
10	-168.96(82)	0.18
12	-227.3(1.5)	0.18

ical result is $\nu=1.00 \pm 0.02$, in perfect agreement with exact analytical results. However, due to the limited scope of the 2D investigation the statistical error is rather large.

IV. SUMMARY AND CONCLUSIONS

By two entirely different lines of approach we have calculated consistent estimates of the critical exponent ν for the 3D Ising model. Averaging over (2.18) and (3.12) gives

$$\nu=0.6303 \pm 0.0014, \quad (4.1)$$

this is in agreement with the value (Ref. 21) $\nu=0.629 \pm 0.004$, and with other results of the extensive literature, see for instance Refs. 32. The methods explored by this study are also suitable for treating other models and problems in statistical mechanics, as well as in lattice-gauge theories.

ACKNOWLEDGMENTS

We would like to thank Roman Salvador and Claus Vohwinkel for providing valuable help. Most of the Monte Carlo data were produced on Florida State University's ETA¹⁰s. This research project was partially funded by the Department of Energy under Contract Nos. DE-FG05-87ER40319 and DE-FC05-85ER2500. Nelson Alves was supported by the Conselho Nacional de Desenvolvimento Científico e Tecnológico (CNPq), Brazil.

¹C. N. Yang and T. D. Lee, Phys. Rev. **87**, 404 (1952); **87**, 410 (1952).

²M. E. Fisher, in *Critical Phenomena*, Proceedings of the 51st Enrico Fermi Summer School, Varena, edited by M. S. Green (Academic, New York, 1972).

³H. W. Blöte and M. P. Nightingale, Physica **112A**, 405 (1982).

⁴E. Brezin, J. Phys. (Paris) **43**, 15 (1982), and references therein; V. Privman and E. Fisher, J. Stat. Phys. **33**, 385 (1983), and references therein.

⁵R. B. Pearson, Phys. Rev. B **16**, 6285 (1982).

⁶C. Itzykson, R. B. Pearson, and J. B. Zuber, Nucl. Phys. **B220** [FS8], 415 (1983).

⁷Z. W. Salsburg, J. D. Jackson, W. Fickett, and W. W. Wood, J.

Chem. Phys. **30**, 65 (1959); D. A. Chesnut and Z. W. Salsburg, *ibid.* **38**, 2861 (1963); I. R. McDonald and K. Singer, Discuss. Faraday Soc. **43**, 40 (1967); J. P. Valleau and D. N. Card, J. Chem. Phys. **57**, 5457 (1972).

⁸K. Binder, J. Comp. Phys. **59**, 1 (1985); R. H. Swendsen and A. M. Ferrenberg (unpublished).

⁹M. Falcioni, E. Marinari, M. L. Paciello, G. Parisi, and B. Taglienti, Phys. Lett. **108B** (1982).

¹⁰E. Marinari, Nucl. Phys. **B235** [FS11], 123 (1984).

¹¹G. Bhanot, S. Black, P. Carter, and R. Salvador, Phys. Lett. B **183**, 331 (1987).

¹²G. Bhanot, R. Salvador, S. Black, P. Carter, and R. Toral, Phys. Rev. Lett. **59**, 803 (1987), and references therein.

- ¹³M. Creutz, *Phys. Rev. Lett.* **50**, 1411 (1983).
- ¹⁴A. M. Ferrenberg and R. Swendsen, *Phys. Rev. Lett.* **61**, 2635 (1988); **63**, 1195 (1989).
- ¹⁵B. Baumann and B. Berg, *Phys. Lett.* **164B**, 131 (1985).
- ¹⁶B. Efron, *SIAM Rev.* **21**, 460 (1979), and references therein.
- ¹⁷B. Berg and A. Billoire, *Phys. Rev. D* **40**, 550 (1989), and references therein.
- ¹⁸R. Villanova (unpublished).
- ¹⁹B. Berg, A. Billoire, and C. Rebbi, *Ann. Phys. (N.Y.)* **142**, 185 (1982); **146**, 470 (1982); K. Ishikawa, M. Teper, and G. Schierholz, *Phys. Lett.* **110B**, 399 (1982).
- ²⁰B. Berg, R. Villanova, and C. Vohwinkel, *Phys. Rev. Lett.* **62**, 2433 (1989).
- ²¹G. S. Pawley, R. H. Swendsen, D. J. Wallace, and K. G. Wilson, *Phys. Rev. B* **29**, 4030 (1984).
- ²²G. Bhanot, D. Duke, and R. Salvador, *J. Stat. Phys.* **44**, 985 (1986).
- ²³B. Berg, A. Billoire, and R. Salvador, *Phys. Rev. D* **37**, 3774 (1988).
- ²⁴B. L. van der Waerden, *Mathematical Statistics* (Springer, New York, 1969).
- ²⁵W. Press *et al.*, *Numerical Recipes* (Cambridge University Press, London, 1986).
- ²⁶G. Münster, *Nucl. Phys.* **B190** [FS3], 439 (1981); **B205** [FS5], 648E (1982).
- ²⁷B. Berg and K. Decker (unpublished).
- ²⁸M. Lüscher, *Cargèse lectures 1983*, edited by G. 't Hooft *et al.* (Plenum, New York, 1984); *Commun. Math. Phys.* **104**, 177 (1986).
- ²⁹M. N. Barber, R. B. Pearson, D. Toussaint, and J. L. Richardson, *Phys. Rev. B* **32**, 1720 (1985).
- ³⁰G. Parisi and F. Rapuano, *Phys. Lett.* **157B**, 301 (1985).
- ³¹G. Kalle and S. Wansleben, *Comput. Phys. Commun.* **33**, 343 (1984).
- ³²J. Zinn-Justin, *J. Phys. (Paris)* **42**, 783 (1981); J. Adler, M. Moshe, and V. Privman, *Phys. Rev. B* **26**, 3958 (1982); M. E. Fisher and J.-H. Chen, *J. Phys. (Paris)* **46**, 1645 (1985); A. J. Liu and M. E. Fisher, *Physica A* **156**, 35 (1989).